Carbohydrate Polymers **6** (1986) 213–244

A Polymer Physico-Chemical Approach to the Study of Commercial Starch Hydrolysis Products (SHPs)

Harry Levine and Louise Slade

General Foods Corporation, Technical Center T22-1, 555 South Broadway, Tarrytown, New York 10591, USA

(Received: 6 February 1986)

SUMMARY

The behavior of 55 commercial SHPs, of dextrose equivalent (DE) 0·3–100, was studied by a low-temperature differential scanning calorimetry technique. The method, based on derivative thermograms, is used to measure the characteristic sub-zero glass transition temperature, T_g', of a maximally freeze-concentrated aqueous solution. An inverse linear correlation exists between T_g' and DE. A plot of T_g' vs. number-average molecular weight ($\bar{M}_n$) demonstrated the classical behavior of SHPs as a homologous series of amorphous glucose polymers, and revealed an 'entanglement coupling' capability for SHPs of $\leqslant 6$ *DE* and $T_g' \geqslant -8°C$. *The possible relationship between intermolecular entanglement (leading to network formation) and SHP functional behavior as a food ingredient in applications involving gelation, encapsulation, frozen-storage stabilization, thermomechanical stabilization or facilitation of drying processes is discussed. The utility of low-DE SHPs for inhibiting various 'collapse'-related phenomena, which affect the processing/storage stability of many foods, is described and explained. An example of the inhibition of enzymic activity in a frozen system, stabilized with low-DE maltodextrin, is cited. A generalized mechanism for collapse is proposed, based on the occurrence of a critical structural relaxation transition at T_g', followed by viscous flow in the rubbery liquid state. The mechanism is derived from Williams–Landel–Ferry free volume theory for amorphous polymers, and leads to a conclusion of the fundamental equivalence of T_g' (or other relevant glass transition temperature, T_g) and the*

Carbohydrate Polymers 0144-8617/86/$03.50 —

observed collapse temperature and the temperature of recrystallization.

INTRODUCTION

The physico-chemical properties of commercial starch hydrolysis products (SHPs), e.g. dextrins, maltodextrins, corn syrup solids, corn syrups, represent an important, but sparsely researched, subject within the food industry (Murray & Luft, 1973). Much can be learned about the functional attributes of SHPs as ingredients in fabricated food products, from a polymer physico-chemical approach to studies of the thermomechanical properties of these amorphous, water-soluble polymers of glucose. For example, To & Flink (1978) demonstrated a correlation between increasing measured collapse temperature, T_c, and increasing number-average degree of polymerization, $\overline{DP}_n$, for an extensive series of SHPs of $2 \leqslant \overline{DP}_n \leqslant 16$ (calculated % dextrose equivalent, $DE^* = 52{\cdot}6$ to $6{\cdot}9$).

Recently reported studies from our laboratories have utilized thermal analysis methods such as differential scanning calorimetry (DSC), dynamic mechanical analysis (DMA) and thermomechanical analysis (TMA) to illustrate and characterize the polymer-chemical properties of various food ingredients and products (e.g. rice and starch (Maurice *et al.*, 1985; Slade, 1984; Slade & Levine, 1984), gelatin (Levine & Slade, 1984*a*; Slade & Levine, 1984) and frozen aqueous sugar and other solutions (Levine & Slade, 1984*b*; Schenz *et al.*, 1984)), all of which behave as systems of amorphous or partially crystalline polymers, oligomers and monomers, soluble in and/or plasticized by water (Sears & Darby, 1982).

We now report a DSC study of the characteristic sub-zero second-order glass transition temperatures (where $T_g = T_g'$) of 55 commercial SHPs with *DE* values in the range 0·3–100. (As defined by Franks (1982), T_g' is the glass transition temperature of the maximally freeze-concentrated solute matrix surrounding the ice crystals in a frozen solution.) This analysis yields a linear correlation between decreasing

* *DE* is defined by eqn (1), since the reducing sugar content (in terms of the number of reducing end groups) of a known weight of sample is compared to an equal weight of glucose of *DE* 100 and $\bar{M}_n$ 180·16.

DE and increasing T_g', such that one could predict a *DE* value for an 'unknown' SHP from its measured T_g', by interpolation using a calibration curve of T_g' vs. *DE* for SHP 'standards' of known *DE*. The same DE/T_g' data have been used to construct a predictive map of functional attributes for SHPs, based on a demonstration of their classical T_g vs. number-average molecular weight ($\bar{M}_n$) behavior as a homologous series of amorphous glucose polymers. The present study examines a more extensive range of SHPs and provides a theoretical basis for interpreting the previously cited results of To & Flink (1978).

The possibility that SHP functional behavior can be predicted from the correlation between *DE* (or $\overline{DP}_n$ or $\bar{M}_n$) and T_g has important implications for a better understanding of the mechanism of various 'collapse'-related phenomena (discussed in recent reviews by Flink (1983) and Karel & Flink (1983)), which affect the processing and storage stability of many fabricated and natural food systems, including frozen products, amorphous dry powders and candy glasses. We shall discuss the potential (and frequently demonstrated) utility of SHPs in preventing structural collapse, as predictable from the present method, within the context of a probable mechanism for the collapse phenomenon. This mechanism is based on the assumption that collapse phenomena are consequences of a structural relaxation process characteristic of the material, which reflects the microscopic and macroscopic manifestations of an underlying and prerequired molecular 'state' transformation from a metastable amorphous solid to liquid which occurs at T_g.

MATERIALS AND METHODS

The SHPs used in this study are listed in Table 1, along with their manufacturers and vegetable sources, wherever known. The majority are typical commercial SHPs, readily available and widely used throughout the food industry, either now or in the past. These materials were analyzed as received, and their *DE* values are those specified by the manufacturers. Glucose and maltose were reagent grade chemicals from Sigma (St Louis, Missouri, USA); maltotriose and maltohexaose were '85% pure' maltooligosaccharide standards from V-Labs (Covington, Louisiana, USA). Three calibrated molecular-weight fractions were also obtained from V-Labs from a

TABLE 1
T_g' Values for Commercial SHPs

SHP	*Manufacturer*	*Source*	*DE*	T_g' (°C)
AB 7436	Anheuser Busch (St Louis, Missouri, USA)	Waxy maize	0·5	−4
Paselli SA-2	AVEBE (Hopelawn, New Jersey, USA)	Potato	2	−4·5
Stadex 9	Staley (Decatur, Illinois, USA)	Dent corn	3·4	−4·5
78NN128	Staley	Potato	0·6	−5
78NN122	Staley	Potato	2	−5
ARD 2326	Amaizo (Hammond, Indiana, USA)	Dent corn	0·4	−5·5
ARD 2308	Amaizo	Dent corn	0·3	−6
AB 7435	Anheuser Busch	Waxy/dent blend	0·5	−6
Star Dri 1	Staley	Dent corn	1	−6
Maltrin M050	GPC (Muscatine, Iowa, USA)	Dent corn	6	−6
Paselli MD-6	AVEBE	Potato	6	−6·5
Dextrin 11	Staley	Tapioca	1	−7·5
MD-6-12	V-Labs		2·8	−7·5
Stadex 27	Staley	Dent corn	10	−7·5
MD-6-40	V-Labs		0·7	−8
Star Dri 5	Staley	Dent corn	5	−8
Paselli MD-10	AVEBE	Potato	10	−8
Morrex 1910	CPC (Englewood Cliffs, New Jersey, USA)	Dent corn	10	−9·5
Star Dri 10	Staley	Dent corn	10	−10
Maltrin M040	GPC	Dent corn	5	−10·5
Frodex 5	Amaizo	Waxy maize	5	−11
Morrex 1918	CPC	Waxy maize	10	−11·5
Maltrin M100	GPC	Dent corn	10	−11·5
Lodex 5	Amaizo	Waxy maize	7	−12
Maltrin M500	GPC	Dent corn	10	−12·5
Lodex 10	Amaizo	Waxy maize	12	−12·5
Maltrin M150	GPC	Dent corn	15	−13·5
MD-6-1	V-Labs		20·5	−13·5
Frodex 15	Amaizo	Waxy maize	18	−14
Frodex 10	Amaizo	Waxy maize	10	−15·5
Lodex 15	Amaizo	Waxy maize	18	−15·5
Maltohexaose	V-Labs		18·2	−15·5
Maltrin M200	GPC	Dent corn	20	−15·5
Maltrin M250	GPC	Dent corn	25	−17·5

TABLE 1— *contd.*

SHP	*Manufacturer*	*Source*	*DE*	T_g' (°C)
Staley 200	Staley	Corn	26	−19·5
Frodex 24	Amaizo	Waxy maize	28	−20·5
DriSweet 36	Hubinger (Keokuk, Iowa, USA)	Corn	36	−22
Maltrin M365	GPC	Dent corn	36	−22·5
Staley 300	Staley	Corn	35	−23·5
Globe 1052	CPC	Corn	37	−23·5
Maltotriose	V-Labs		35·7	−23·5
Frodex 42	Amaizo	Waxy maize	42	−25·5
Neto 7300	Staley	Corn	42	−26·5
Globe 1132	CPC	Corn	43	−27·5
Staley 1300	Staley	Corn	43	−27·5
Neto 7350	Staley	Corn	50	−27·5
Maltose	Sigma		52·6	−29·5
Globe 1232	CPC	Corn	54·5	−30·5
Staley 2300	Staley	Corn	54	−31
Sweetose 4400	Staley	Corn	64	−33·5
Sweetose 4300	Staley	Corn	64	−34
Globe 1642	CPC	Corn	63	−35
Globe 1632	CPC	Corn	64	−35
Royal 2626	CPC	Corn	95	−42
Glucose	Sigma	Corn	100	−43

maltodextrin standard, MD-6, with the following manufacturer's specifications (as measured by high-performance aqueous gel permeation chromatography): MD-6-1, $\bar{M}_n = 880$ and $\bar{M}_w = 1030$; MD-6-12, $\bar{M}_n = 6500$ and $\bar{M}_w = 13\,000$; and MD-6-40, $\bar{M}_n = 27\,200$ and $\bar{M}_w = 39\,300$. For these V-Labs and Sigma samples, *DE* values were calculated, using the equation:

$$DE = 100/(\bar{M}_n/180{\cdot}16) \quad (1)$$

All SHP solutions for T_g' determination were 20% w/w solids basis (i.e. 20·0 g solid solute per 100·0 g solution), in distilled deionized water. Samples were prepared by mechanical stirring, with gentle heating when necessary, to produce clear solutions or homogeneous sols. (Generally, water solubility of SHPs decreases with decreasing *DE* (Murray & Luft, 1973).)

The effect of freezer-storage temperature on enzymic activity was investigated experimentally *in vitro* in a model system consisting of glucose oxidase (from Sigma), glucose, methyl red, and bulk solutions of sucrose, Morrex 1910 (10 *DE* maltodextrin) and their mixtures, which provided a range of samples with known values of T_g'. The enzymic oxidation of glucose produces an acid which turns the reaction mixture from yellow to pink. Samples with a range of T_g' values from $-9{\cdot}5$ to -32°C were stored at various temperatures (25, 3, -15 and -23°C), and monitored for color change over time.

DSC measurements were performed with a DuPont 990 Thermal Analyzer combined with a Model 910 Differential Scanning Calorimeter equipped with a liquid nitrogen quench cooling accessory capable of sample cooling at about 50°C min^{-1}. The analog derivative function on the DuPont 990 allowed the precise determination of transition temperatures, with a reproducibility (for duplicate samples) of $\pm 0{\cdot}5$°C for T_g'. In practice, 20–30 mg of solution were hermetically sealed in an aluminum sample pan, and scanned (against an empty reference pan), at a heating rate of 5°C min^{-1}, from -60°C (or below) to $+25$°C. Initial cooling to below -60°C (in all cases, well below T_g') ensured maximal freeze concentration, and thus maximally frozen samples.

RESULTS

Figure 1 shows two typical low-temperature DSC thermograms for 20% w/w SHP solutions: (A) glucose and (B) Star Dri 10 10*DE* maltodextrin. In each, the heat flow curve begins at the top (endothermic range down) and the derivative trace (zeroed to the temperature axis) at the bottom. For both thermograms, instrumental amplification and sensitivity settings were identical, and sample weights comparable. As illustrated by Fig. 1, the derivative feature of the DuPont 990 greatly facilitates the identification of sequential thermal transitions, assignment of precise transition temperatures, and thus overall interpretation of thermal behavior, especially for such frozen aqueous solutions exemplified by Fig. 1(A) (Schenz *et al.*, 1984). Surprisingly, we could find no other reported use of derivative thermograms, in the many DSC studies of such systems, to sort out the small endothermic and exothermic changes in heat flow that occur typically below 0°C (see Franks (1982) for extensive bibliography).

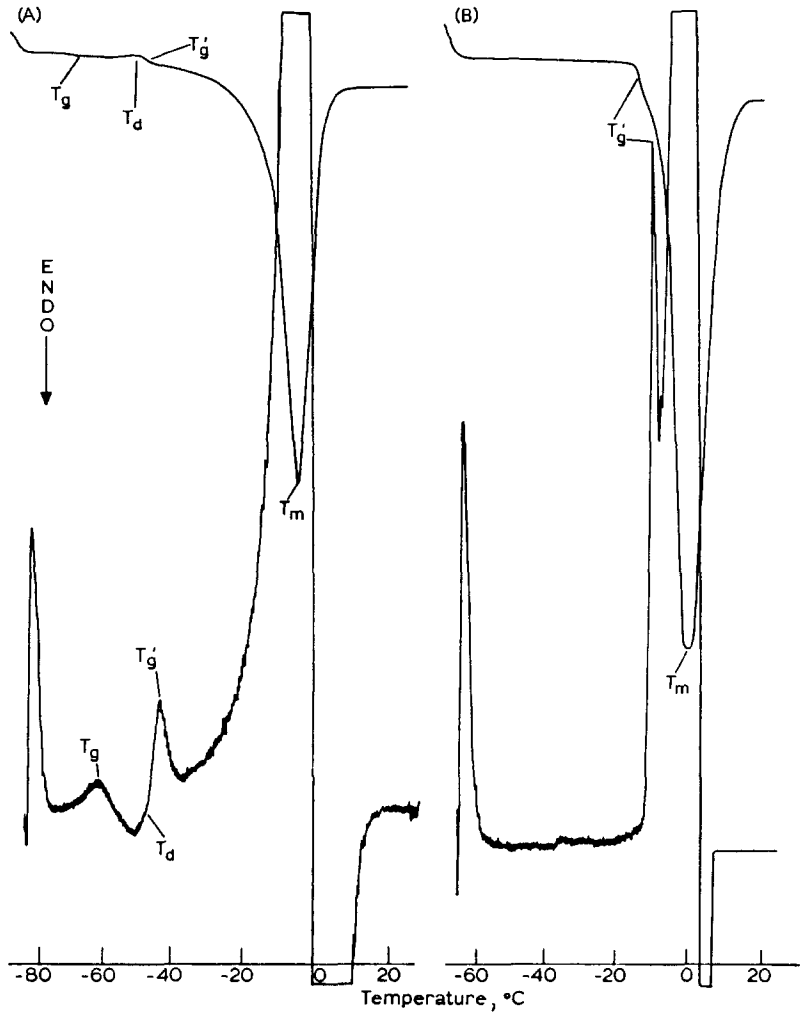

Fig. 1. Typical DSC thermograms for 20% w/w solutions of (A) glucose and (B) Star Dri 10 10 *DE* maltodextrin. In each, the heat flow curve begins at the top (Endothermic range down) and the derivative trace (zeroed to the temperature axis) at the bottom.

Despite the handicap of such instrumental shortcomings in the past, the theoretical basis for the thermal properties manifested by aqueous solutions at sub-zero temperatures has come to be well understood, as described in detail (along with voluminous corroborative experimental results) by, e.g., Franks, MacKenzie and their co-workers (Luyet,

1960; Rasmussen & Luyet, 1969; MacKenzie & Rasmussen, 1972; Franks *et al.*, 1977; MacKenzie, 1977, 1981; Franks, 1982). Hence, only the new and salient features of the present results will be described. In Fig. 1(A), after rapid cooling of the glucose solution to below −80°C, slow heating revealed a minor T_g at −61·5°C, followed by an exothermic devitrification (a crystallization of some of the previously unfrozen water) at −47·5°C, immediately followed by another (major) T_g, namely T_g', at −43°C, and then finally the 'equilibrium' melting of ice at T_m. In Fig. 1(B), the maltodextrin solution thermogram is much simpler, showing only the obvious glass transition at $T_g' = -10$°C, in addition to T_m. These assignments of transitions and temperatures can be definitively reconciled with the appropriate solid–liquid 'state' diagrams, as reported by MacKenzie & Rasmussen (1972 (Fig. 18)) and Franks (1982). In such state diagrams (e.g. Fig. 6 in this paper will be described in the Discussion), the different cooling–heating paths which can be followed by solutions of typical monomeric and polymeric solutes are revealed. For the former (e.g. glucose), partial vitrification of the original dilute solution can occur because the cooling rate is fast relative to the time required for ice crystallization, whereas for the latter (e.g. a maltodextrin) the cooling rate is comparatively lower relative to the time for rapid freezing. However, as demonstrated by the thermograms in Fig. 1, in both cases re-warming forces the system through a major glass transition at T_g'. (Note: In many earlier DSC studies (e.g. MacKenzie (1977, 1981) and Maltini (1977)), performed without the benefit of derivative thermograms, a pair of transition temperatures (independent of initial concentration) called $T_{antemelting}$ and $T_{incipient\ melting}$ have been reported in place of a single T_g'. In fact, in the many cases that we have studied, the reported values of T_{am} and T_{im} bracket that of T_g' as we measure it, leading us to surmise that T_{am} and T_{im} actually represent the temperatures of onset and completion of the single thermal event (a glass transition) that must occur at T_g', as defined by the state diagram.)

The point of greatest interest in the thermograms in Fig. 1 involves T_g' (Schenz *et al.*, 1984). As defined by Franks (1982), T_g' is the T_g of the freeze-concentrated solute matrix surrounding the ice crystals in a maximally frozen solution. This matrix, which is a supersaturated solution of all the solute in the fraction of water remaining unfrozen, exists as a 'metastable' amorphous solid (a glass, of constant composi-

tion) at any temperature below T_g',* but as a viscoelastic liquid (a rubbery fluid) at any temperature between T_g' and T_m. Again, with regard to a state diagram for a typical water-soluble solute that does not readily undergo eutectic crystallization (see Franks (1982), Schenz *et al.* (1984) or Fig. 6 later), T_g' corresponds to the intersection of the thermodynamically defined liquidus curve and the kinetically determined supersaturated glass curve. As such, Franks (1982) described T_g' as a 'metastable eutectic', in that it represents a quasi-invariant point in the state diagram, invariant as to both its characteristic temperature (T_g') and composition (i.e. C_g', herein expressed as a concentration of g unfrozen water/g solute) for a particular solute. (However, 'eutectic' in this case does not imply phase separation.) This glass, which forms, e.g., on slow cooling to T_g', acts as a kinetic barrier to further ice formation (within the experimental time frame), despite the continued presence of unfrozen water at all temperatures below T_g', as well as a barrier to any other diffusion-controlled process. Recognizing this, one begins to appreciate why the temperature of this glass transition is very important in several aspects of frozen food technology, e.g. freezer storage stability, freeze concentration and freeze drying (Franks, 1982), which can involve various recrystallization and 'collapse' phenomena, as will be described in the Discussion.

In Table 1 are listed the measured T_g' values for the 55 commercial SHPs analyzed. The T_g' for glucose of -43°C is midway between reported values for T_{am} and T_{im} (Rasmussen & Luyet, 1969), and within ± 2° of various values for T_c and T_r (recrystallization) (MacKenzie, 1977; Franks, 1982). The same is true of our previously reported T_g' for sucrose of -32°C (Schenz *et al.*, 1984). Elsewhere in the literature are values for T_c and/or T_r (also always independent of initial concentration) for soluble starch of -5 or -6°C (Luyet, 1960; Franks, 1982), and for dextrin of -9°C (Luyet, 1960), which are also comparable to our T_g' values for various dextrins of <1 *DE* and maltodextrins of <10 *DE*, respectively.

Figure 2 shows T_g' plotted vs. *DE* for all the SHPs. There is a reasonable linear correlation between increasing T_g' and decreasing

* The glass at T_g', with invariant composition, has been described in previous literature as 'metastable' (Franks, 1982). More discriminating terminology, e.g. kinetically metastable, will be discussed in a future publication.

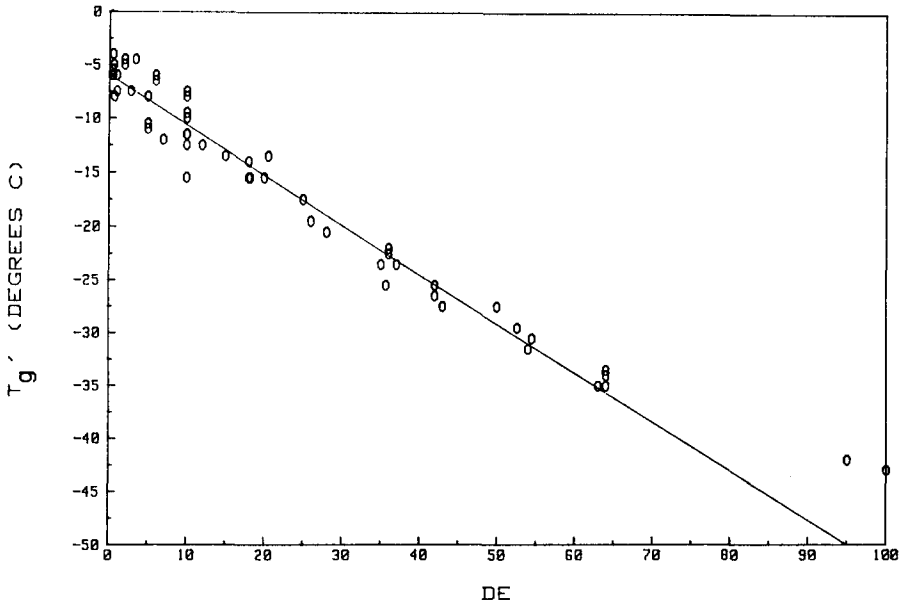

Fig. 2. Variation of the glass transition temperature, T_g', for maximally frozen 20% w/w solutions against *DE* values for 55 commercial SHPs.

DE, as demonstrated by the regression line which has a correlation coefficient $R = -0{\cdot}98$. If we assume, as defined by eqn (1), that *DE* is inversely proportional to $\overline{DP}_n$ and $\bar{M}_n$ for this series of SHPs, then the results in Fig. 2 demonstrate that T_g' increases with increasing $\bar{M}_n$. Such a correlation between T_g and $\bar{M}_n$ is the general rule for any homologous family of synthetic glass-forming monomers, oligomers and polymers (Billmeyer, 1984).

The equation describing the regression line in Fig. 2 is

$$DE = -2{\cdot}2(T_g') - 12{\cdot}9 \qquad (2)$$

We used eqn (2) to calculate *DE* values for three SHPs of unknown *DE* from their measured T_g' values: Crystal Gum, a tapioca dextrin from National Starch (Bridgewater, New Jersey, USA), had a T_g' of -6°C, and a calculated *DE* of <1; Capsul, a modified waxy maize starch from National Starch, a T_g' of $-9{\cdot}5$°C, and a *DE* of 7·6; and MD-6, a maltodextrin whole-polymer standard from V-Labs, a T_g' of $-12{\cdot}5$°C, and therefore a *DE* of 14. Such calculated *DE* values seem

reasonable approximations for a dextrin and a maltodextrin, so that Fig. 2 commends itself as a calibration curve useful for interpolating *DE* values of 'unknown' SHPs. This approximate method, based on eqn (2), may be preferable to the more tedious and time-consuming classical experimental methods for *DE* determination (Murray & Luft, 1973).

Figure 3 shows T_g' plotted vs. C_g' for 13 of the corn syrups, in the *DE* range 26–95, listed in Table 1. The composition of the glass at T_g' was calculated from the thermogram, specifically from the measurement of the area (enthalpy) under the ice melting endotherm. By calibration with pure water, this measurement yields a maximum weight of ice in the frozen sample, and, by difference from the known weight of total water in the initial solution, a weight of unfrozen water, per unit weight of solute, in the glass at T_g'. Many in the food industry will recognize this procedure as one of several routine methods for determining what is referred to as the 'water binding capacity' of a solute.

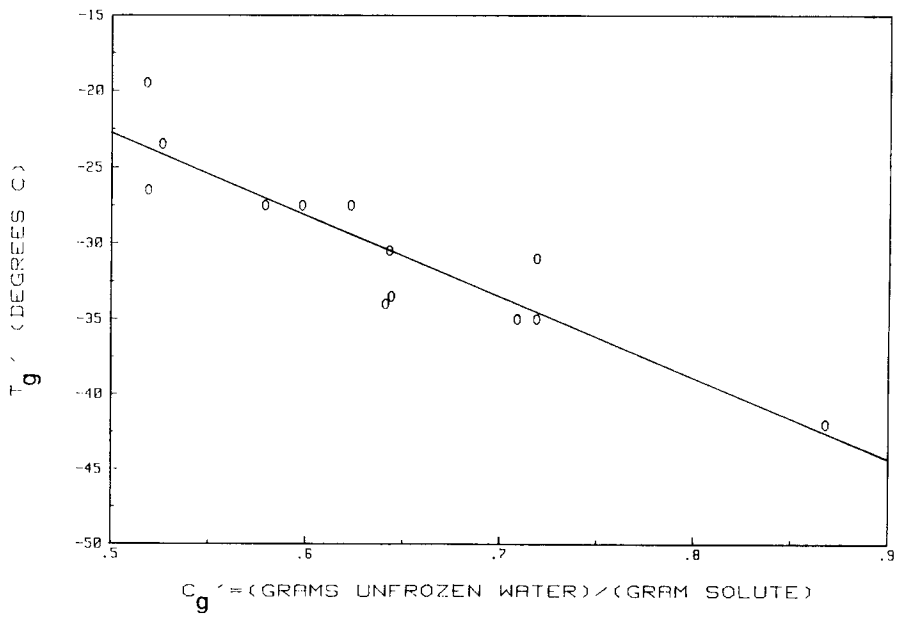

Fig. 3. Variation of the glass transition temperature, T_g', for maximally frozen 20% w/w solutions against C_g', the composition of the glass at T_g', in g unfrozen water per g solute, for 13 commercial corn syrups.

Franks (1982) has reviewed this subject in detail, and taken great pains to point out that this so-called 'bound' water is not truly bound in any energetic sense. It has been shown to be subject to rapid exchange, and to have thermally labile hydrogen bonds, cooperative molecular mobility, a heat capacity, C_p, approximately equal to that of liquid water rather than ice and some capability to dissolve salts (as reviewed by Levine & Slade (1984*b*)). Furthermore, it has been demonstrated, for water-soluble polymers and monomers alike, that such unfreezability of water is not due to tight binding by solute but to kinetic (non-equilibrium) retardation effects on the diffusion of water and solute molecules at the low temperatures approaching the vitrification T_g of the solute/unfrozen water mixture (Franks, 1982).

As shown by the results in Fig. 3, C'_g (expressed as g unfrozen water/g solute) decreases with increasing T'_g for this series of corn syrup solids solutions. (The correlation coefficient for the linear regression line is $-0{\cdot}91$.) In other words, as the average $\bar{M}_n$ of the solute(s) increases, the fraction of the total water unfrozen in the glass at T'_g generally decreases. This fact is also illustrated dramatically by the thermograms in Fig. 1. For comparable amounts of total water, the area under the ice melting peak for the glucose solution is much smaller than that for the maltodextrin solution. Once again, in the context of a typical state diagram (e.g. Fig. 6), the above results show that as the average $\bar{M}_n$ of the water-soluble solute(s) in an aqueous system increases, the T'_g/C'_g point generally moves up the temperature axis toward 0°C and to the right along the composition axis toward 100 w% solute. The critical importance of this fact will become clear in the Discussion, where we describe SHP functional behavior *vis-à-vis* T'_g, and the possibilities of inhibiting collapse phenomena by formulating a fabricated food product with the intent of elevating T'_g.

DISCUSSION

Insights into structure/property relations for SHPs

At first glance, the straightforward presentation of the *DE* vs. T'_g data in Fig. 2 does not appear to be the most rigorous theoretical treatment. Yet the linear correlation of *DE* with T'_g and the convenience for practical application in the estimation of *DE* to characterize SHP

samples seem to justify its potential use. The rigorous theoretical dependence of DE on T_g' stems from the respective dependence of each of these parameters on the degree of linear polymerization and molecular weight (MW) within a series of monodisperse (i.e. MW = $\bar{M}_n$ = weight-average MW, $\bar{M}_w$) homopolymers. High polymers can be distinguished from oligomers because of their capacity for molecular chain 'entanglement coupling', resulting in the formation of rubber-like viscoelastic random networks (often called gels, in accord with Flory's nomenclature for disordered three-dimensional networks formed by physical aggregation (Flory, 1953, 1974)) above a critical polymer concentration (Ferry, 1980). As summarized by Mitchell (1980), 'entanglement coupling is seen in most high MW polymer systems. Entanglements (in gels) behave as crosslinks with short lifetimes. They are believed to be topological in origin rather than involving chemical bonds.' For linear homopolymers (either amorphous or partially crystalline, and not necessarily monodisperse) with $\bar{M}_n$ values below the entanglement limit, there is a theoretical linear decrease in T_g with increase in $1/\bar{M}_n$ (Billmeyer, 1984). The onset of entanglement corresponds to a plateau region in which further increases in MW have little or no effect on T_g (Billmeyer, 1984). (There may, however, be a dramatic effect on the viscoelastic properties of the network, resulting, e.g., in increased gel strength at constant temperature (Ferry, 1980).) The conventional presentation of such experimental data is simply T_g vs. $\bar{M}_w$ (Billmeyer, 1984), which conveniently displays the plateau region. Two typical examples are shown in Fig. 4. The main plot describes the behavior of a homologous series of amorphous linear poly(vinyl acetate) samples, commercially available as Vinnapas PVAc's from Wacker-Chemie (Berghauser, FRG) (which provided the $\bar{M}_w$ values). The plateau region, which includes high polymer samples that demonstrate viscoelastic rheological properties, is clearly observed (Levine & Slade, 1984*b*). In the inset of Fig. 4 is shown an idealized figure (from a Perkin-Elmer DSC user's manual (Brennan, 1973)) illustrating the generalized relationship between T_g and $\bar{M}_w$. As exemplified in Fig. 4, T_g increases monotonically with increasing $\bar{M}_w$ up to the plateau limit for the region of entanglement coupling (typically at $\bar{M}_w$ somewhere in the range 10^4–10^5 daltons (Billmeyer, 1984)), then levels off.

To a first approximation, DE has the simple inverse dependence on $\bar{M}_n$ defined by eqn (1). Expressing eqn (1) in the form $\bar{M}_n = 18\,016/$

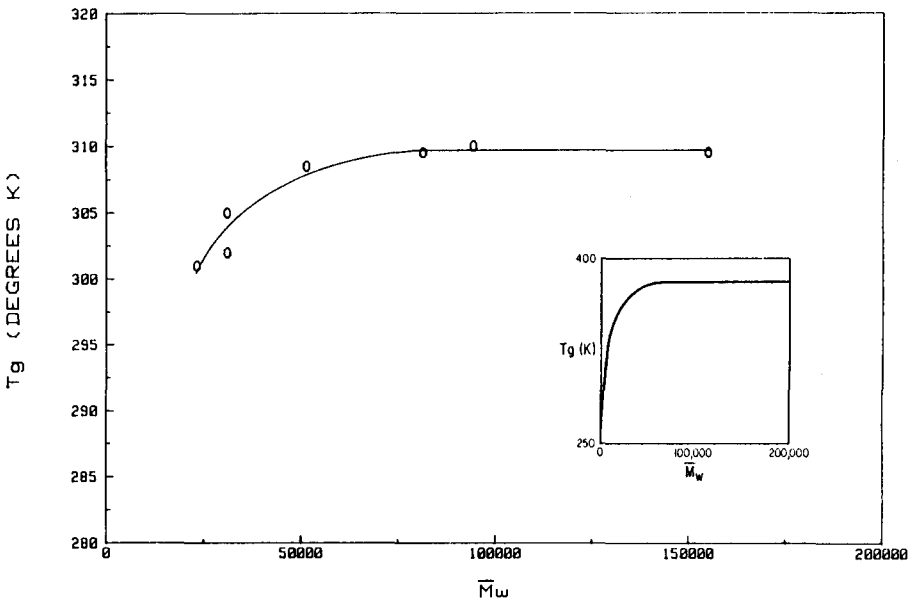

Fig. 4. Variation of the glass transition temperature, T_g, against $\bar{M}_w$ for a series of commercial poly(vinyl acetate) polymers (from Levine & Slade (1984*b*)). (Inset: an idealized plot of T_g vs. $\bar{M}_w$ (Brennan, 1973).)

DE, and using the conventional presentation to explore the behavior of T_g' with MW, we show in the main plot of Fig. 5 the T_g' results for the 55 commercial SHPs. After a steeply rising portion, a plateau region is reached for SHPs with $DE \leqslant 6$ *and* $T_g' \geqslant -8°C$.* The most likely explanation for this previously unreported behavior is that such SHPs experience molecular entanglement in the freeze-concentrated glass that exists at T_g' and C_g'. Consequently, SHP samples with $DE \leqslant 6$ and $T_g' \geqslant -8°C$ should be capable of forming gel networks (via entanglement), at concentrations above a critical polymer concen-

* In the inset of Fig. 5 is shown the theoretical linear decrease in T_g' with increase in $1/\bar{M}_n$, for SHPs with $\bar{M}_n$ values below the entanglement limit. To & Flink's (1978) T_c/MW data (Fig. 4, p. 574, in their paper) showed the same correlation. In fact, the theoretical treatment of the data in the inset is simply a modified version of the straightforward presentation in Fig. 2, with the same correlation coefficient $r = -0{\cdot}98$.

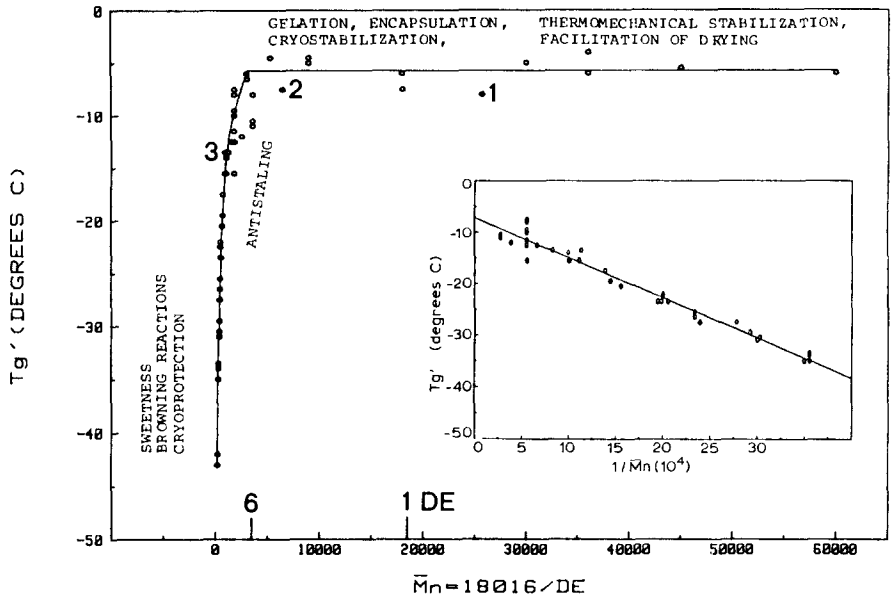

Fig. 5. Variation of the glass transition temperature, T_g', against $\bar{M}_n$ (expressed as a function of *DE*) for 55 commercial SHPs. *DE* values are indicated by the numbers marked above the *x*-axis. Data points for the maltodextrin MW standards are numbered 1, 2 and 3 to provide molecular weight markers. Areas of specific functional attributes, corresponding to three regions of the diagram, are labelled. (Inset: a plot of T_g' vs. $1/\bar{M}_n \times 10^4$ for SHPs with $\bar{M}_n$ values below the entanglement limit, illustrating the theoretically predicted linear dependence.)

tration (related to C_g'). Braudo *et al.* (1984), in their reports of the viscoelastic properties of thermoreversible maltodextrin gels (at $T > 0°C$), have also implicated entanglement coupling above a critical polymer concentration. They have concluded that the non-cooperative gelation behavior shown by maltodextrins is characteristic of semi-rigid chain polymers. This is consistent with Ferry's (1980) observation that 'molecules which are relatively stiff and extended (in concentrated solution) exhibit the effects of entanglement coupling even more prominently than do highly flexible polymers'. Additional information about thermoreversible maltodextrin (5–8 *DE*) gels comes from Bulpin *et al.* (1984), who have reported that such SHP gels are apparently composed of a network of high MW (> 10 000)

branched molecules derived from amylopectin. These branched molecules represent the structural elements, which are aggregated with, and further stabilized by interactions with, short linear chains (MW < 10 000) derived from amylose.

The possible implications of our new finding and the conclusions we draw from it may be important in helping to explain previously observed but poorly understood aspects of SHP functional behavior in various food-related applications. The SHPs which fall on the plateau region in Fig. 5 have *DE* values from 6 to 0·3. Based on eqn (1), these *DE* values correspond to $\overline{DP}_n$ values in the range 18–370, respectively, and $\bar{M}_n$ values between 3000 and 60 000. (The data points for the three maltodextrin MW standards are indicated in Fig. 5 to provide MW markers. The points for (1) MD-6-40 ($\bar{M}_n = 27\,200$; $\bar{M}_w = 39\,300$) and (2) MD-6-12 ($\bar{M}_n = 6500$; $\bar{M}_w = 13\,000$) fall on the plateau, while (3) MD-6-1 ($\bar{M}_n = 880$; $\bar{M}_w = 1030$) is below the entanglement limit.) Within this series of commercial SHPs, the minimum linear chain length apparently required for intermolecular entanglement corresponds to $DP_n \simeq 18$ and $\bar{M}_n \simeq 3000$. This fact explains why no plateau region was observed in To & Flink's (1978) plot of T_c vs. $\overline{DP}_n$ for SHPs of $\overline{DP}_n \leqslant 16$ and $DE \geqslant 6{\cdot}9$. Their Fig. 3 (on p. 573) and the portion of our Fig. 5 for $DE \geqslant 7$ are extremely similar in appearance, in that both show a steeply rising portion for $DE \geqslant 20$, followed by a less steeply rising portion for $20 \geqslant DE \geqslant 7$. The entanglement capability evidenced by just such SHPs of $DE \leqslant 6$ (materials not previously studied by the polymer characterization method described herein) may therefore underlie various important aspects of their functional behavior. For example, as shown by Slade's (1984) review of the literature, sufficiently long linear chain lengths ($DP_n \gtrsim 18$) of SHPs have been correlated with intermolecular network formation and thermoreversible gelation, and with SHP and starch (re)crystallization by a chain-folding mechanism. It may be that, in a partially crystalline SHP gel network, the coexistence of random interchain entanglements in the amorphous regions and chain-folded microcrystalline junction zones comprising the crystalline regions represents concomitant (but *not* necessarily cause-and-effect) consequences of a sufficiently long chain length. This suggestion is supported by the recent work of Ellis & Ring (1985) and Miles *et al.* (1985), who reported that amylose gels, which are found to be partially crystalline, form on cooling solutions of molecularly

entangled chains. The latter workers stated that amylose gelation requires network formation, and this network formation requires entanglement, and they concluded that 'polymer entanglement is important in understanding the gelation of amylose'.

The excellent fit of the experimental data in Fig. 5 to the conventional presentation of the behavior expected for such a family of oligomers and high polymers is gratifying, especially considering the numerous caveats that one must mention about commercial SHPs. For example, Fig. 5 was constructed using $\bar{M}_n$ (and implicitly $\overline{DP}_n$), calculated from *DE*, while the conventional form (Fig. 4) utilizes $\bar{M}_w$ as a basis for specifying a typical MW range for the entanglement limit. Furthermore, for highly polydisperse solutes such as commercial SHPs (for which MW distribution, MWD = $\bar{M}_w/\bar{M}_n$, is frequently a variable), T_g' is rigorously dependent on the average $\bar{M}_w$ of a mixture of solute molecules (Franks, 1982). Despite these facts, the entanglement limit of $\bar{M}_n \simeq 3000$ for the SHPs in Fig. 5 is within the characteristic range of 1250–19000 for the entanglement MWs of many typical synthetic linear high polymers (Graessley, 1984).

Other largely uncontrollable potential variables within the series of SHPs include the following: (a) significant sample variability in solids composition (i.e. saccharides distribution) for a single SHP, which would affect the reproducibility of T_g'; and (b) 'as is' moisture contents (in the generally specified range of 5–10%) for different solid SHPs, which would not affect measured T_g' (since, e.g., 15, 20 and 25% w/w solutions would all freeze-concentrate to the same invariant T_g' point in the state diagram), but would affect the calculated C_g'. Hence, the C_g' data in Fig. 3 were only those for some commercial corn syrups, whose moisture contents are generally more tightly specified. Another origin of variability among different commercial SHPs of nominally comparable *DE* concerns the method of production, e.g. hydrolysis by acid, enzyme or acid plus enzyme (Murray & Luft, 1973). Especially with regard to enzymic hydrolysates, each particular enzyme used leads to a different set of characteristic breakdown products with a unique MWD (Krusi & Neukom, 1984). Still another major variable among different SHPs from different vegetable starch sources involves the original amylose/amylopectin ratio for a starch, and the consequent ratio of linear to branched polymer chains in an SHP. This variable can be particularly pronounced among a set of low-*DE* maltodextrins (which would contain higher-*DP* fractions),

some from linear amylose-containing dent corn and some from all-amylopectin (branched) waxy maize. The consequent range of T_g' values can be pronounced as well, since, as a generally observed rule, linear chains give rise to higher T_g' than branched chains of the same $\bar{M}_w$. This type of behavior is exemplified by the T_g' data for the eight 10 *DE* maltodextrins listed in Table 1, where T_g' ranges from $-7{\cdot}5$°C for Stadex 27 from dent corn to $-15{\cdot}5$°C for Frodex 10 from waxy maize, a ΔT of 8°C. The obvious conclusion regarding a suitable maltodextrin for a specific application is that one SHP is not necessarily interchangeable with another of the same nominal *DE*, but from a different commercial source. Basic characterization of structure/property relations, e.g. in terms of T_g' (rather than *DE*, which can be a less significant, even misleading parameter), is often advisable before selecting such food ingredients.

Predicted functional attributes of SHPs

Further insights into the structure/function relationships for SHPs may be gleaned, if one considers Fig. 5 as a predictive map of areas of functional behavior for SHP samples. For example, SHPs which fall on the entanglement plateau can be postulated to demonstrate certain functional attributes, some of which have already been verified in the past, but not quantitatively explained from a theoretical basis such as the entanglement capability revealed by the present study. Thus, it appears (as described below) that the plateau region defines the useful range of gelation, encapsulation, cryostabilization, thermomechanical stabilization and facilitation of drying processes. The lower end of the $\bar{M}_n$ range corresponds to the area of sweetness, browning reactions and cryoprotection. The intermediate region at the upper end of the steeply rising portion represents the area of anti-staling ingredients. The map (so labelled as in Fig. 5) can be used to choose individual SHPs or mixtures of SHPs and other carbohydrates (e.g. targeted to a particular T_g' value) to achieve desired complex functional behavior for specific product applications.

As a specific example, the synthesis of SHPs capable of gelation from solution should be designed to yield materials of $DE \leqslant 6$ *and* $T_g' \geqslant -8$°C. This prediction is in good agreement with the results of Richter and co-workers (Richter *et al.*, 1976*a*, *b*; Braudo *et al.*, 1979),

who reported that 25% w/w solutions of potato starch maltodextrins of 5–8 *DE* produced thermoreversible, fat-mimetic gels, and with those of Lenchin *et al.* (1985), who patented tapioca SHPs of $DE < 5$ which also form fat-mimetic gels from solution. Commercial maltodextrins to be used for effective encapsulation of volatile flavors/aromas and lipids should likewise be capable of entanglement and network formation (i.e. $T_g' \geqslant -8°C$). As reported by Flink and coworkers (To & Flink, 1978; Flink, 1983; Karel & Flink, 1983), effectiveness of encapsulation increases with increasing T_c, which in turn increases with increasing $\overline{DP}_n$ within a series of SHPs, although 'a quantitative relationship between T_c and MW has not been established' (To & Flink, 1978, p. 572).

With regard to the freezer-storage (in other words 'cryo') stabilization of fabricated frozen food products (e.g. desserts such as ice cream, with a smooth, creamy texture) against ice crystal growth over time, the inclusion of low-*DE* maltodextrins would elevate the composite T_g' of the mix of soluble solutes, which is typically dominated by low-MW sugars. As a result, one would observe, in practice, a retarded rate of ice recrystallization ('grain growth') at the characteristic freezer temperature (T_f), along with an increase of the phenomenological T_r. Such behavior has been documented in the soft-serve ice cream patents of Cole *et al.* (1983, 1984) and Holbrook & Hanover (1983). In such products, ice recrystallization is known to involve a diffusion-controlled maturation process with a mechanism analogous to 'Ostwald ripening', whereby larger crystals grow with time at the expense of smaller ones which eventually disappear (Maltini, 1977; Bevilacqua & Zaritzky, 1982; Harper & Shoemaker, 1983). The rate of such a process, at T_f, would be reduced, as would also be the $\Delta T (= T_f - T_g')$, by formulating with low-*DE* maltodextrins of high T_g'.

Low-*DE* maltodextrins and other high-MW polymeric solutes are well known as drying aids for processes such as freeze, spray and drum drying (To & Flink, 1978; MacKenzie, 1981; Flink, 1983; Karel & Flink, 1983; Szejtli & Tardy, 1985). Through their elevating effect on the composite T_g', and their parallel effect of reducing the unfrozen water fraction at C_g' for freeze drying (or on other relevant T_g/C_g for spray or drum drying), maltodextrins raise the observed T_c (at any particular % moisture) relative to the drying temperature, thus facilitating drying without collapse or 'melt-back'.

Thermomechanical stabilization refers to the stabilization of, e.g., candy glasses against such collapse phenomena as recrystallization of sugars ('graining'), mechanical deformation and stickiness. Here, too, it has been shown by White & Cakebread (1966), Vink & Deptula (1982) and Lees (1982) that inclusion of low-*DE* maltodextrins in low-MW sugar glasses (to increase average $\bar{M}_w$ of solutes) increases T_g, thus increasing storage stability at $T < T_g$. Even when such a candy 'melt' is in the rubbery state at $T_g < T_{storage}$, maltodextrins are known to function as inhibitors of the diffusion-controlled propagation step in the recrystallization process (White & Cakebread, 1966).

For the lower-T_g' SHPs in Fig. 5, sweetness and browning reactions are salient functional attributes. A less familiar one involves the potential for cryoprotection of biological materials (Franks, 1982). The map predicts that such SHPs and other low-MW carbohydrates, in sufficiently concentrated solution, can be quench-cooled to a completely vitrified state, wherein all the water is captured in the solute/unfrozen water glass. If such a glass were maintained below its T_g, and served as the external medium for cells previously suspended in the SHP solution, extracellular ice formation and the concomitant cellular damage resulting from lethal osmotic effects might be avoided through such a method of cryoprotection.* The essence of this cryoprotective function, avoidance of ice formation by concentrated solutions of low-MW solutes which have high C_g' values, also has a readily apparent relationship to food applications involving soft, spoonable or pourable-from-the-freezer products. One recent example is Rich's patented 'Freeze-Flo' beverage concentrate formulated with high fructose corn syrup (Kahn & Eapen, 1982).

The literature on SHPs as anti-staling ingredients for starch-based food products (reviewed by Slade (1984)), including the recent work of Krusi & Neukom (1984), shows that (non-entangling) SHP oligomers of $\overline{DP}_n$ 3–8 are effective in inhibiting, *and* not participating in, starch recrystallization.

One could also postulate from the map of Fig. 5 that addition of a low-MW sugar to a gelling maltodextrin should produce a sweet and softer gel. Addition of a glass-forming sugar to an encapsulating

* Such a process would require rapid mixing as well as cooling of the suspended cells in the cryoprotectant solution, so that the total time spent above T_g would be insufficient to allow cell dehydration due to the osmotic stress.

maltodextrin should enhance the collapse of the entangled network around the adsorbed species (if collapse were desirable), but decrease the ease of spray drying. Furthermore, the map leads to two other intriguing postulates. The freeze-concentrated glass at T_g' of an effective SHP cryostabilizer ($\leqslant 6$ *DE*) would contain entangled solute molecules, while in the glass at T_g' of an SHP cryoprotectant the solute molecules would not be entangled. By analogy, various high-MW polysaccharide gums have been reported to be capable of improving freezer-storage stability of ice-containing foods in a poorly understood manner. The effect has been attributed to increased viscosity (Keeney & Kroger, 1974; Harper & Shoemaker, 1983). Such gums may owe their success not only to their viscosity-increasing ability, which is common to all glass-formers, but to their possible capability to undergo molecular entanglement in the freeze-concentrated, non-ice matrix of the frozen food. Entanglement might further enhance their ability to inhibit diffusion-controlled processes. In a related vein, the effects of entanglement coupling on the viscoelastic and rheological properties of random coil polysaccharide concentrated solutions (Morris *et al.*, 1981) and gels (Mitchell, 1980; Braudo *et al.*, 1984), at temperatures above 0°C, have been discussed recently.

The role of SHPs in collapse-related phenomena and their mechanism of action

In the rest of this Discussion, we explore the critical role of SHPs in preventing structural collapse, within a context of the various collapse-related phenomena listed in Table 2. These phenomena include those pertaining to processing and/or storage at temperatures above 0°C as well as ones involving the frozen state, all of which are governed by the particular T_g relevant to the system and its content of plasticizing water. While for frozen systems T_g' of the freeze-concentrated glass is the relevant T_g for describing the T_g/MW relationship (as illustrated by Fig. 5), for amorphous dried powders and candy glasses the relevant T_g pertains to a higher temperature/lower moisture state. It has been tacitly assumed that a plot of T_g vs. $\bar{M}_n$ for 'dry' SHPs would reflect the same fundamental behavior as that shown in Fig. 5. In fact, since T_c for low-moisture samples represents a good quantitative approximation of dry T_g, To & Flink's (1978) results substantiate this assumption.

TABLE 2
Collapse-Related Phenomena which are Governed by T_g and Involve Plasticization by Water (Reference Numbers in Square Brackets Correspond to Numbered References within the Reference List)

	References
I. Processing and/or storage at $T > 0°C$	
(1) Cohesiveness, sticking, agglomeration, sintering, lumping, caking and flow of amorphous powders $\geqslant T_{collapse}$	[4], [5], [8], [11], [18], [21], [22], [23], [26], [27], [28], [30]
(2) Plating of, e.g., coloring agents on surfaces of amorphous powder particles $\geqslant T_g$	[31]
(3) (Re)crystallization in amorphous powders $\geqslant T_{collapse}$	[5], [11], [18], [27], [30]
(4) Structural collapse in freeze-dried products (after sublimation phase) $\geqslant T_{collapse}$	[5], [11], [27], [28]
(5) Loss of encapsulated volatiles in freeze-dried products (after sublimation phase) $\geqslant T_{collapse}$	[4], [5], [11], [25], [27]
(6) Oxidation of encapsulated lipids in freeze-dried products (after sublimation phase) $\geqslant T_{collapse}$	[5], [27]
(7) Enzymic activity in amorphous solids $\geqslant T_g$	[1], [19]
(8) Stickiness in spray drying and drum drying $\geqslant T_{sticky\ point}$	[4], [5], [11], [27], [28]
(9) Graining in boiled sweets $\geqslant T_g$	[2], [5], [9], [10], [12], [15], [24], [29], [30]
(10) Sugar bloom in chocolate $\geqslant T_g$	[3], [20]
II. Processing and/or storage at $T < 0°C$	
(1) Ice recrystallization ('grain growth') $\geqslant T_{recrystallization}$	[6], [7], [14], [17]
(2) Lactose crystallization ('sandiness') in dairy products $\geqslant T_{recrystallization}$	[5], [6], [30]
(3) Enzymic activity $\geqslant T_g'$	[13], [19]
(4) Structural collapse, shrinkage or puffing (of amorphous matrix surrounding ice crystals) during freeze drying (sublimation phase) = 'melt-back' $\geqslant T_{collapse}$	[5], [6], [11], [14], [16], [27], [28], [30]
(5) Loss of encapsulated volatiles during freeze drying (sublimation phase) $\geqslant T_{collapse}$	[5], [11], [25], [27]

The extensive recent literature on the caking of amorphous or partially crystalline food powders and on the other related phenomena listed in Table 2 (see references therein) leads us to conclude that all these phenomena are consequences of a collapse-type structural relaxation. These various consequences represent the micro-

scopic and macroscopic manifestations of an underlying and prerequisite second-order transformation from amorphous solid (i.e. glass) to amorphous liquid (i.e. rubber), which occurs at T_g. All the phenomena in Table 2 (as well as the glass transition itself (Ferry, 1980)) are diffusion-controlled (many are also nucleation-limited) processes, which are driven by a mechanism involving viscous flow (Flink, 1983), under conditions of $T > T_g$ and viscosity $\eta \lesssim \eta_g = 10^{11}$–$10^{14}$ Pa s (Downton *et al.*, 1982). These kinetic processes are controlled by the superposed dependent variables of time, T and % moisture (Tsourouflis *et al.*, 1976). At the transformation temperature, % H_2O is the critical determinant of collapse and its concomitant changes (Karel & Flink, 1983), through the effect of water on T_g. This plasticizing effect of increasing moisture content at constant T (≡ the effect of increasing T at constant % H_2O) leads to increased segmental mobility of polymer chains in the amorphous regions of both glassy and partially crystalline polymers. This in turn leads to the occurrence of the glass transition at decreased T (Cakebread, 1969).

The above concepts are well-illustrated by the state diagram for poly(vinyl pyrrolidone)–water, shown in Fig. 6. Poly(vinyl pyrrolidone) (PVP) is a much studied water-miscible, amorphous polymer whose behavior in association with water represents a good model of the analogous behavior of polymeric SHPs. The state diagram for water–PVP ($\bar{M}_n = 10^4$, $4{\cdot}4 \times 10^4$ and 7×10^5, as specified by the manufacturer) in Fig. 6, compiled from several literature references (MacKenzie & Rasmussen, 1972; Franks *et al.*, 1977; MacKenzie, 1977; Olson & Webb, 1978; Franks, 1982) and augmented with our measurements of T'_g and dry T_g (Levine & Slade, 1984*b*), is the most complete one presently available for this polymer. It clearly illustrates the dramatic effect of water on T_g, such that the T_g curve ranges from 100°C for dry PVP-44 to ~ −135°C for glassy water (Franks, 1982).

Whenever the glass transition and the resultant collapse phenomenon share a common time frame (Franks, 1982), T_g equals the minimum onset temperature for all the collapse-related phenomena in Table 2. Thus, a system is stable against collapse, within the time period of the experimental measurements of T_g and T_c, at $T < T_g$. Increasing % H_2O leads to decreased stability and shelf-life, at a particular storage temperature (Karel & Flink, 1983). The various phenomenological threshold temperatures (e.g. $T_c \simeq T_r \simeq T_{\text{sticky point}}$) are all equal to the particular T_g (or T'_g) which corresponds to the solute(s)

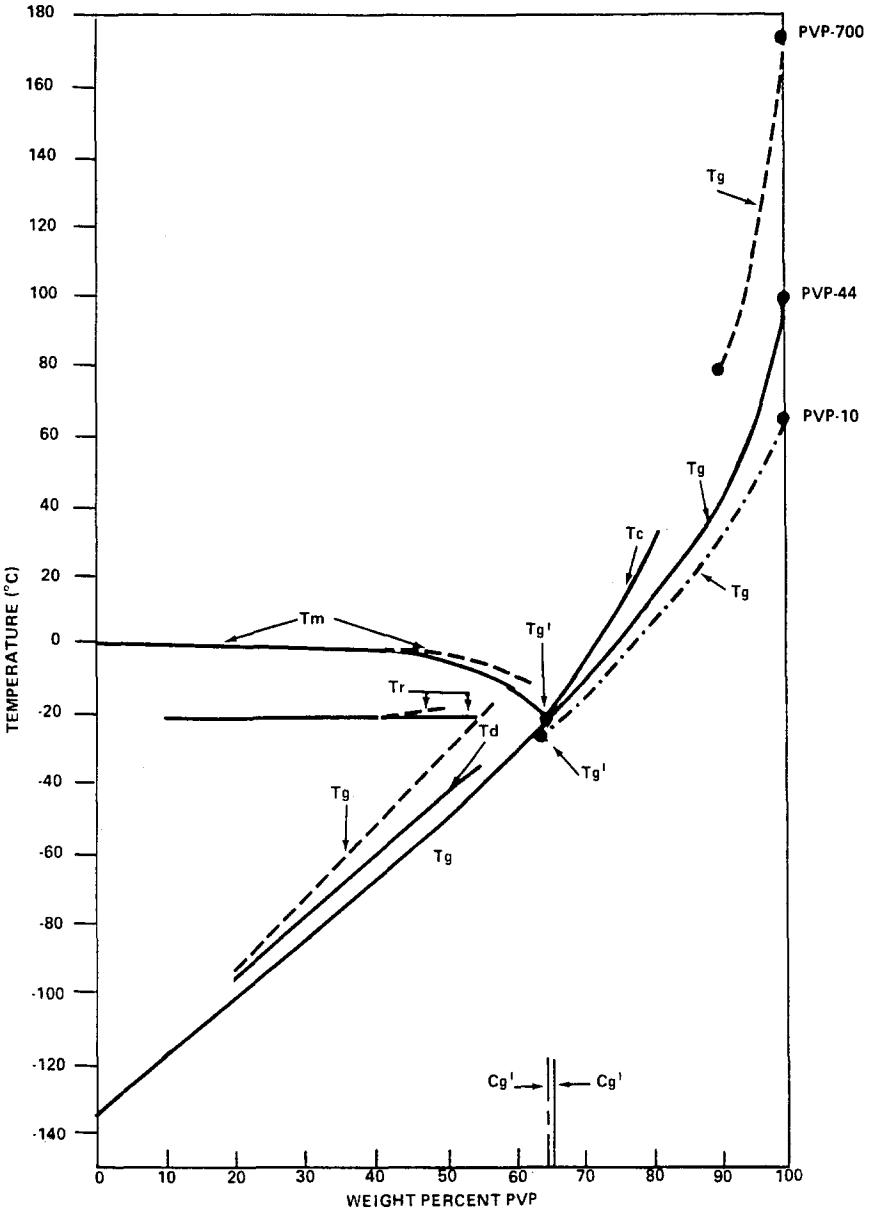

Fig. 6. Solid–liquid state diagram for water–PVP, showing the following transitions: T_m, T_g, T_g', T_d, T_r, T_c. Key: ——, PVP-44; - - - - -, PVP-700; —·—·—, PVP-10; ●- - -●, data of Olson & Webb (1978); other ● refer to data of Levine & Slade (1984*b*).

concentration for the situation in question. Again illustrating with Fig. 6, for PVP-44, $T'_g = T_r = T_c \simeq -21{\cdot}5°C$ and $C'_g \simeq 0{\cdot}54$ g unfrozen water per g PVP (MacKenzie & Rasmussen, 1972; MacKenzie, 1977; Franks, 1982; Levine & Slade, 1984*b*), while for PVP-700 $T_g = T_c = T_{sp} \simeq 120°C$ at $\simeq 5\%$ residual moisture (Olson & Webb, 1978; Levine & Slade, 1984*b*). The equivalence of T_r for ice or solute recrystallization, T_c for collapse, and the concentration-invariant T'_g for an ice-containing system explains why the phenomenological T_r and T_c have always been observed in the past to be concentration-independent for all initial solute concentrations lower than C'_g (Franks, 1982), as illustrated in Fig. 6.

Our conclusion regarding the *fundamental* equivalence of T_g, T_c and T_r represents a departure from the previous literature. For example, while To & Flink (1978) acknowledged that 'the relationship between T_c and MW is identical to the equation for T_g of mixed polymers' and that 'collapse and glass transition are (clearly) phenomenologically similar events', they differentiated between T_g and T_c by pointing out that 'while glass transitions in polymeric materials are generally reversible, the collapse of freeze dried matrices is irreversible'. While the latter facts may be true, the argument is misleading. At the molecular level, the glass-to-rubber transition for a thermoplastic material is reversible. For example, the glass at T'_g/C'_g can be repeatedly warmed and recooled (slowly) over a completely reversible T/C path between its solid and liquid states. The same is true for a completely amorphous (and non-crystallizable) freeze-dried material. The reason collapse is said to be irreversible for a porous matrix has nothing to do with reversibility between molecular states. Irreversible loss of porosity is simply a macroscopic, morphological consequence of viscous flow in the rubbery state at $T > T_g$, whereby the porous glass relaxes to a fluid, incapable of supporting its own weight against flow, which then becomes non-porous and more dense. Subsequent recooling to $T < T_g$ yields a non-porous glass of the original composition, which can thereafter be temperature-cycled reversibly. The only irreversible aspect of T_g-governed collapse is loss of porosity.

A physico-chemical mechanism for collapse based on WLF theory

A universally applicable, quantitative physico-chemical mechanism for collapse-related phenomena is provided by the

Williams-Landel-Ferry (WLF) free volume theory for the temperature dependence of the viscoelastic properties of amorphous polymers and glass-forming liquids within the temperature range for the rubbery (supercooled liquid) state from T_g to $T_g + 100°C$ (Ferry, 1980). The WLF equation, derived from free volume theory, describes the kinetic nature of the glass transition, and defines the exponential temperature dependence of the rate of any diffusion-controlled relaxation process, e.g. η, occurring at T, vs. the rate at a reference temperature T_g below T, in terms of $\log \eta_T/\eta_g \propto \Delta T$, where $\Delta T = T - T_g$ (Ferry, 1980). The WLF equation depends critically on the appropriate reference T_g (for a particular glass-forming system, be it T_g' for a frozen system or T_g for a low-moisture one), which is defined as an iso-free volume state and approximately as an iso-viscosity state of $\eta_g \simeq 10^{11}$–10^{14} Pa s (Soesanto & Williams, 1981).

The impact of WLF-governed behavior on the rates of diffusion-controlled relaxation processes in amorphous polymer–water systems (e.g. structural collapse, ice recrystallization) can be illustrated by the following relative rates (vs. rate = 1 at $T = T_g$, or $\Delta T = 0$) calculated from the WLF equation (Ferry, 1980): for $\Delta T = 3$, 7, 11 and 21°C, rate = 10, 10^2, 10^3 and 10^5, respectively. These calculations would also apply, e.g., to retardation of the rate of the propagation step in the mechanism of recrystallization of an amorphous but crystallizable polymer (or monomer), where the rate would be zero at $T < T_g$ (i.e. immobility ≡ inhibition of migratory diffusion of large main chain segments), but would increase exponentially with increasing ΔT above T_g. In some collapse phenomena, such a recrystallization transition (from amorphous liquid to crystalline solid) may occur after the glass transition (White & Cakebread, 1966), and its rate would be likewise defined by the WLF equation.

The controlled agglomeration of amorphous powders represents a specific example of a WLF-governed process related to caking. As reported by Downton *et al.* (1982), and substantiated by the recent work of Tardos *et al.* (1984), *spontaneous* agglomeration of solid powder particles occurs when η of the liquid phase at the surface of the particle drops to $\sim 10^7$ Pa s. This η is $\sim 10^5$ lower than η_g at T_g. From the WLF equation, this $\Delta\eta$ of 10^5 Pa s corresponds to a ΔT of $\sim 21°C$ between T_g and the T_{sp} for spontaneous agglomeration. Thus, on a typical state diagram of T vs. % moisture, the T_g and T_{sp} curves would represent parallel iso-viscosity lines. The T_{sp} curve for *fast*

agglomeration during processing (reported by Downton *et al.*, 1982) would lie above the T_g curve for *slow* caking during storage, and the ΔT of 21°C would reflect the different operational time scales for the two phenomena.

Based on WLF theory, our physico-chemical mechanism for collapse would be described as follows. As T rises above T_g (or as T_g falls below T, due to water plasticization of a hygroscopic glass), polymer free volume increases. This leads to increased segmental mobility, which allows η to fall below the η_g range of 10^{11}–10^{14} Pa s. As a result, the glass-to-rubber transition occurs, thus permitting viscous liquid flow. In this liquid state, translational diffusion is no longer inhibited, and diffusion-controlled relaxations are free to proceed with rates governed by the WLF equation, i.e. log rate $\propto \Delta T$ (Downton *et al.*, 1982). Referring again to the state diagram in Fig. 6, one sees that a T_g curve corresponds to a boundary between physical states in which the collapse-related phenomena in Table 2 either can (at $T > T_g$) or cannot (at $T < T_g$) occur over realistic times, and that the WLF equation defines the rates of various molecular relaxation processes that will occur above T_g, in terms of an exponential function of ΔT above this boundary condition.

In practice, collapse (and all its different manifestations) can be prevented, and product quality and stability maintained, by the following two fundamental countermeasures: (1) storage at $T < T_g$ (White & Cakebread, 1966); and (2) formulation to increase T_g to a temperature above the processing or storage temperature, by increasing the overall $\bar{M}_w$ of the water-soluble solutes in a product mixture. As has been described, the latter can often be accomplished by adding polymeric stabilizers such as the lower-*DE* SHPs to a formulation dominated by low-MW sugars (Maltini, 1974). The effect of increased MW on the T_g of PVPs is likewise evident in Fig. 6.

Prevention of enzymic activity at $T < T_g$

One collapse-related phenomenon listed in Table 2 but not previously discussed involves enzymic activity, in amorphous substrate-containing media, which occurs only at $T > T_g$. Enzymic activity represents a pleasing case study with which to close this discussion, because it is potentially important in many food applications which cover the entire spectrum of processing/storage temperatures and moisture con-

tents, and because examples exist which elegantly illustrate the fact that activity is inhibited in low-moisture amorphous solids at $T < T_g$, and in frozen systems at $T < T_g'$. Bone & Pethig (1982) studied the hydration of dry lysozyme powder at 20°C, and found that at 20% w/w water the lysozyme was sufficiently plasticized to permit measurable enzymic activity to commence. We interpreted their results to indicate the following: a diffusion-controlled enzyme/substrate interaction is essentially prohibited in a glassy solid at $T < T_g$, but sufficient water plasticization depresses the T_g of lysozyme to < 20°C, allowing the onset of enzymic activity in the lysozyme solution at $T > T_g$, the threshold T for activity (Levine & Slade, 1984*b*). Morozov & Gevorkian (1985) also recently noted the critical importance of low-temperature, water-plasticized glass transitions to the physiological functionality of lysozyme and other globular proteins.

Within the context of cryostabilization, and the potentially critical role of low-*DE* SHPs as cryostabilizers, we have verified the above conclusion in maximally frozen biological systems at $T \ll 0$°C. By analogy, in such cases, the threshold temperature for onset of enzymic activity would be T_g'. Cryostabilization, as a potential technology, is a means of protecting freezer-stored and freeze-dried foods from the deleterious changes in texture (e.g. grain growth of ice, solute crystallization), structure (e.g. shrinkage, collapse) and chemical composition (e.g. flavor degradation, fat rancidity, as well as enzymic reactions) typically encountered. The key to this protection lies in controlling the physico-chemical properties of the freeze-concentrated matrix surrounding the ice crystals. If this matrix is maintained as a mechanical solid (at $T_f < T_g'$), then the diffusion-controlled changes that typically result in reduced storage stability can be prevented or at least greatly retarded. If, on the other hand, a natural food is improperly stored at too high a T_f, or a fabricated product is improperly formulated, and thus the matrix is allowed to exist in the freezer as a rubbery fluid (at $T_f > T_g'$), then freezer storage stability would be reduced. Furthermore, the rates of the various deleterious changes would increase exponentially with the ΔT between T_f and T_g', as dictated by the WLF theory.

The prevention of enzymic activity at temperatures below T_g' was demonstrated experimentally *in vitro* in a model system consisting of glucose oxidase, glucose, methyl red, and bulk solutions of sucrose, Morrex 1910 (10 *DE* maltodextrin) and their mixtures, which pro-

vided a range of samples with known values of T_g'. The enzymic oxidation of glucose produces an acid which turns the reaction mixture from yellow to pink. Samples with a range of T_g' values from $-9{\cdot}5$ to $-32°C$ were stored at various temperatures: 25°C, 3°C, $-15°C$ and $-23°C$. All of the samples were fluid at the two higher temperatures, while all looked like colored blocks of ice at $-15°C$ and $-23°C$. However, only the samples for which $T_{storage}$ was above T_g' turned pink! Even after 2 months storage at $T_f = -23°C$, the samples containing the maltodextrin, with $T_g' > -23°C$, were still yellow. The frozen samples which turned pink, even at $-23°C$, contained a concentrated enzyme-rich fluid surrounding the ice crystals, while in those which remained yellow the non-ice matrix was a glassy solid. Significantly, enzymic activity was prevented by storage below T_g', but the enzyme itself was not inactivated. When the yellow samples were thawed, they quickly turned pink. Thus, cryostabilization with a low-*DE* SHP preserved the enzyme during frozen storage, but prevented its activity below T_g'.

ACKNOWLEDGEMENTS

We thank our colleagues at General Foods, T. W. Schenz and T. J. Maurice, for their contributions to the research program from which the present work derives; our consultant, Professor Felix Franks of the University of Cambridge, for invaluable discussions and encouragement; and L. Hofmann and S. Goldfarb for excellent technical assistance.

REFERENCES*

Bevilacqua, A. E. & Zaritzky, N. E. (1982). *J. Food Sci.* **47**, 1410.

Billmeyer, F. W. (1984). *Textbook of polymer science*, 3rd edn, New York, Wiley-Interscience.

Bone, S. & Pethig, R. (1982). *J. Mol. Biol.* **157**, 571. [1]

Braudo, E. E., Belavtseva, E. M., Titova, E. F., Plashchina, I. G., Krylov, V. L., Tolstoguzov, V. B., Schierbaum, F. R. & Richter, M. (1979). *Staerke* **31**, 188.

Braudo, E. E., Plashchina, I. G. & Tolstoguzov, V. B. (1984). *Carbohydr. Polym.* **4**, 23.

*Reference numbers in square brackets correspond to references cited in Table 2.

Brennan, W. P. (1973). *Thermal analysis application study No. 8*, Norwalk, Perkin Elmer Instrument Division.
Bulpin, P. V., Cutler, A. N. & Dea, I. C. M. (1984). In *Gums and stabilizers for the food industry*, Vol. 2, eds G. O. Phillips *et al.*, Oxford, Pergamon Press, p. 475.
Cakebread, S. H. (1969). *Manufact. Confect.* **49** (8), 41. [2]
Chevalley, J., Rostagno, W. & Egli, R. H. (1970). *Rev. Internat. Chocolat* **25**, 3. [3]
Cole, B. A., Levine, H. I., McGuire, M. T., Nelson, K. J. & Slade, L. (1983). US Patent 4,374,154, 15 February 1983.
Cole, B. A., Levine, H. I., McGuire, M. T., Nelson, K. J. & Slade, L. (1984). US Patent 4,452,824, 5 June 1984.
Downton, G. E., Flores-Luna, J. L. & King, C. J. (1982). *Indust. Engn. Chem. Fund.* **21**, 447. [4]
Ellis, H. S. & Ring, S. G. (1985). *Carbohydr. Polym.* **5**, 201.
Ferry, J. D. (1980). *Viscoelastic properties of polymers*, 3rd edn, New York, John Wiley & Sons.
Flink, J. M. (1983). In *Physical properties of foods*, eds M. Peleg and E. B. Bagley, Westport, AVI Publ., p. 473. [5]
Flory, P. J. (1953). *Principles of polymer chemistry*, Ithaca, Cornell University Press.
Flory, P. J. (1974). *Faraday Discuss. Chem. Soc.* **57**, 7.
Franks, F. (1982). In *Water: a comprehensive treatise*, Vol. 7, ed. F. Franks, New York, Plenum Press, p. 215. [6]
Franks, F., Asquith, M. H., Hammond, C. C., Skaer, H. B. & Echlin, P. (1977). *J. Microsc.* **110** (3), 223. [7]
Fukuoka, E., Kimura, S., Yamazaki, M. & Tanaka, T. (1983). *Chem. Pharmaceut. Bull.* **31** (1), 221. [8]
Graessley, W. W. (1984). In *Physical properties of polymers*, eds J. E. Mark *et al.*, Washington, DC, American Chemical Society, p. 97.
Gueriviere, J. F. (1976). *Indust. Aliment. Agric.* **93** (5), 587. [9]
Harper, E. K. & Shoemaker, C. F. (1983). *J. Food Sci.* **48**, 1801.
Herrington, T. M. & Branfield, A. C. (1984). *J. Food Technol.* **19**, 409. [10]
Holbrook, J. L. & Hanover, L. M. (1983). US Patent 4,376,791, 15 March 1983.
Kahn, M. L. & Eapen, K. E. (1982). US Patent 4,332,824, 1 June 1982.
Karel, M. & Flink, J. M. (1983). In *Advances in drying*, Vol. 2, ed. A. S. Mujumdar, Washington, DC , Hemisphere Publ., p. 103. [11]
Keeney, P. G. & Kroger, M. (1974). In *Fundamentals of dairy chemistry*, 2nd edn, eds B. H. Webb *et al.*, Westport, AVI Publ., p. 890.
Krusi, H. & Neukom, H. (1984). *Staerke* **36**, 300.
Lees, R. (1982). *Confect. Product.*, February, 50. [12]
Lenchin, J. M., Trubiano, P. C. & Hoffman, S. (1985). US Patent 4,510,166, 9 April 1985.
Levine, H. & Slade, L. (1984*a*). In *Royal Society of Chemistry — Water soluble polymers: chemistry &application technology course manual*, 16–20 July, Girton College, Cambridge, p. 274.

Levine, H. & Slade, L. (1984*b*). In *Royal Society of Chemistry — Water soluble polymers: chemistry &application technology course manual*, 16–20 July, Girton College, Cambridge, p. 259. [13]
Luyet, B. (1960). *Ann. NY Acad. Sci.* **85**, 549.
MacKenzie, A. P. (1977). *Phil. Trans. Roy. Soc. Lond. B.* **278**, 167. [14]
MacKenzie, A. P. (1981). In *Microprobe analysis of biological systems*, New York, Academic Press, p. 397.
MacKenzie, A. P. & Rasmussen, D. H. (1972). In *Water structure at the water–polymer interface*, ed. H. H. G. Jellinek, New York, Plenum Press, p. 146.
McNulty, P. B. & Flynn, D. G. (1977). *J. Text. Stud.* **8**, 417. [15]
Maltini, E. (1974). *ADISVTPA* **5**, 65. [16]
Maltini, E. (1977). *IIF–IIR-Karlsruhe* **1**, 1. [17]
Maurice, T. J., Slade, L., Sirett, R. R. & Page, C. M. (1985). In *Properties of water in foods*, eds D. Simatos and J. L. Multon, Dordrecht, Martinus Nijhoff Publ., p. 211.
Miles, M. J., Morris, V. J. & Ring, S. G. (1985). *Carbohydr. Res.* **135**, 257.
Mitchell, J. R. (1980). *J. Text. Stud.* **11**, 315.
Moreyra, R. & Peleg, M. (1981). *J. Food Sci.* **46**, 1918. [18]
Morozov, V. N. & Gevorkian, S. G. (1985). *Biopolymers* **24**, 1785. [19]
Morris, E. R., Cutler, A. N., Ross-Murphy, S. B. & Rees, D. A. (1981). *Carbohydr. Polym.* **1**, 5.
Murray, D. G. & Luft, L. R. (1973). *Food Technol.* **27** (3), 32.
Niediek, E. A. & Barbernics, L. (1981). *Gordian* **80** (11), 267. [20]
Olson, D. R. & Webb, K. K. (1978). *Org. Coat. Plast. Chem.* **39**, 518.
Passy, N. & Mannheim, C. H. (1982). *Lebensm.-Wiss. u.-Technol.* **15**, 222. [21]
Peleg, M. & Mannheim, C. H. (1977). *J. Food Process. Preserv.* **1**, 3. [22]
Rasmussen, D. & Luyet, B. (1969). *Biodynamica* **10**, 319.
Richter, M., Schierbaum, F., Augustat, S. & Knoch, K. D. (1976*a*). US Patent 3,962,465, 8 June 1976.
Richter, M., Schierbaum, F., Augustat, S. & Knoch, K. D. (1976*b*). US Patent 3,986,890, 19 October 1976.
Rosenzweig, N. & Narkis, M. (1981). *Polym. Engn. Sci.* **21** (17), 1167. [23]
Schenz, T. W., Rosolen, M. A., Levine, H. & Slade, L. (1984). In *Proceedings of the 13th NATAS Conference*, ed. A. R. McGhie, 23–26 September, Philadelphia, Pennsylvania, p. 57.
Sears, J. K. & Darby, J. R. (1982). *The technology of plasticizers*, New York, Wiley-Interscience.
Slade, L. (1984). *American Association of Cereal Chemists 69th Annual Meeting*, Minneapolis, Minnesota, 30 September–4 October, No. 112.
Slade, L. & Levine, H. (1984). In *Proceedings of the 13th NATAS Conference*, ed. A. R. McGhie, 23–26 September, Philadelphia, Pennsylvania, p. 64.
Soesanto, T. & Williams, M. C. (1981). *J. Phys. Chem.* **85**, 3338. [24]
Szejtli, J. & Tardy, M. (1985). US Patent 4,529,608, 16 July 1985. [25]
Tardos, G., Mazzone, D. & Pfeffer, R. (1984). *Can. J. Chem. Engn.* **62**, 884. [26]

To, E. C. & Flink, J. M. (1978). *J. Food Technol.* **13**, 551. [27]
Tsourouflis, S., Flink, J. M. & Karel, M. (1976). *J. Sci. Food Agric.* **27**, 509. [28]
Vink, W. & Deptula, R. W. (1982). US Patent 4,311,722, 19 January 1976. [29]
White, G. W. & Cakebread, S. H. (1966). *J. Food Technol.* **1**, 73. [30]
Wuhrmann, J. J., Venries, B. & Buri, R. (1975). US Patent 3,920,854, 18 November 1975. [31]

NOTE

After this manuscript was written, our conclusion about the fundamental equivalence of T_g', T_r and T_c was corroborated by Reid. He reported a study (Reid, D. S. (1985). *Cryo-Letters* **6**, 181) in which T_g', measured by DSC, corresponded well with the temperature at which a frozen aqueous system, viewed under a cryomicroscope, became physically mobile. Reid remarked that 'T_g', the temperature at which a system would be expected to become mobile due to the appearance of the solution phase, has also been related to the collapse temperature in freeze drying, again relating to the onset of system mobility, which presumably allows for the diffusion of solution components'. Reid's study reveals another collapse-related phenomenon, governed by T_g' of a frozen system, that can be added to Table 2: slow warming of cryopreserved embryos to $T > T_g'$ facilitates the detrimental diffusion of ionic components (salts), resulting in cellular damage due to high ionic strength, and in much reduced embryo survival.